The Plant Cell, Vol. 18, 3218–3234, November 2006, www.plantcell.org

Insights into Nuclear Organization in Plants as Revealed by the Dynamic Distribution of *Arabidopsis* SR Splicing Factors [W]

Vinciane Tillemans,[a] Isabelle Leponce,[a] Glwadys Rausin,[a] Laurence Dispa,[a] and Patrick Motte[a,b,1]

[a] Laboratory of Plant Cell and Molecular Biology, Department of Life Sciences, Institute of Botany, University of Liège, B-4000 Liège, Belgium

[b] Center for Assistance in Technology of Microscopy, Department of Chemistry, University of Liège, B-4000 Liège, Belgium

Serine/arginine-rich (SR) proteins are splicing regulators that share a modular structure consisting of one or two N-terminal RNA recognition motif domains and a C-terminal RS-rich domain. We investigated the dynamic localization of the *Arabidopsis thaliana* SR protein RSZp22, which, as we showed previously, distributes in predominant speckle-like structures and in the nucleolus. To determine the role of RSZp22 diverse domains in its nucleolar distribution, we investigated the subnuclear localization of domain-deleted mutant proteins. Our results suggest that the nucleolar localization of RSZp22 does not depend on a single targeting signal but likely involves different domains/motifs. Photobleaching experiments demonstrated the unrestricted dynamics of RSZp22 between nuclear compartments. Selective inhibitor experiments of ongoing cellular phosphorylation influenced the rates of exchange of RSZp22 between the different nuclear territories, indicating that SR protein mobility is dependent on the phosphorylation state of the cell. Furthermore, based on a leptomycin B– and fluorescence loss in photobleaching–based sensitive assay, we suggest that RSZp22 is a nucleocytoplasmic shuttling protein. Finally, with electron microscopy, we confirmed that RSp31, a plant-specific SR protein, is dynamically distributed in nucleolar cap-like structures upon phosphorylation inhibition. Our findings emphasize the high mobility of *Arabidopsis* SR splicing factors and provide insights into the dynamic relationships between the different nuclear compartments.

INTRODUCTION

The large majority of protein-coding genes in eukaryotes are transcribed as long precursor molecules containing intervening sequences (or introns), which are excised by a macromolecular and dynamic edifice, termed the spliceosome, to form the mature mRNA. The spliceosome consists of the five small nuclear ribonucleoproteins (snRNPs) U1, U2, U4/U6, and U5 and a plethora of non-snRNP–associated splicing factors, including serine/arginine-rich (SR) proteins (reviewed in Jurica and Moore, 2003; Patel and Steitz, 2003). These proteins are key components of the nuclear machinery regulating different aspects of pre-mRNA splicing, including the assembly of the spliceosome through both protein–protein and protein–RNA interactions. Significantly, SR proteins bind to exonic splicing enhancers and promote the recruitment of the heterodimeric splicing factor U2AF and the U1 snRNP to the 3′ and 5′ splice sites, respectively. SR proteins are also known to play a role in alternative pre-mRNA splicing by determining alternative splice site selection (Graveley, 2000; van Der Houven Van Oordt et al., 2000; Cazalla et al., 2005; Matlin et al., 2005). In mammals, 10 SR proteins have been described with sizes ranging from 20 to 75 kD (Bourgeois et al., 2004). They are characterized by a modular organization generally consisting of an N-terminal domain with one or two RNA recognition motifs (RRMs) and a C-terminal domain rich in Ser and Arg residues, hence termed the RS domain. The RRM domain is thought to determine RNA binding specificity, whereas the RS domain is involved mainly in protein–protein interactions. SR proteins are regulated by reversible phosphorylation, which appears to be required for spliceosome assembly and for coupling splicing with downstream cellular processes, such as mRNA localization, export, stability, and translation efficiency (Huang and Steitz, 2001; Lemaire et al., 2002; Huang et al., 2003; Lai and Tarn, 2004; Sanford et al., 2004, 2005; Zhang and Krainer, 2004).

In the interphase nucleus, SR proteins are localized primarily in irregularly shaped domains, termed nuclear speckles, that correspond to interchromatin granule clusters and perichromatin fibrils in electron microscopy (Sacco-Bubulya and Spector, 2002). Speckles are thought to act as storage, assembly, and/or modification sites from which splicing factors are recruited to perform pre-mRNA splicing at the transcription sites. The relocation of mammalian SR proteins from speckles to actively transcribed genes has been shown to depend on their phosphorylation status (Melcak et al., 2000; Misteli, 2000). It is becoming apparent that eukaryotic cells regulate gene expression by spatially organizing the molecular machinery involved in the many nuclear events that include splicing. Furthermore, in mammalian cells, a

[1] To whom correspondence should be addressed. E-mail patrick.motte@ulg.ac.be; fax 32-4366-2960.
The author responsible for distribution of materials integral to the findings presented in this article in accordance with the policy described in the Instructions for Authors (www.plantcell.org) is: Patrick Motte (patrick.motte@ulg.ac.be).
[W] Online version contains Web-only data.
www.plantcell.org/cgi/doi/10.1105/tpc.106.044529

subset of SR proteins, such as ASF/SF2, 9G8, and SRp20, shuttle continuously between the nucleus and the cytoplasm (Caceres et al., 1998). These SR proteins associate with mRNA, providing an adapter function in recruiting the export receptor TAP/Nuclear Export Factor1 (Huang et al., 2003, 2004; Huang and Steitz, 2005).

Recent analyses of the *Arabidopsis thaliana* and rice (*Oryza sativa*) genomes have identified at least 19 and 20 genes, respectively, encoding distinct SR-related proteins belonging to several subclasses (Kalyna and Barta, 2004; Isshiki et al., 2006). Some SR proteins are homologous to the human prototypes ASF/SF2, SC35, and 9G8, whereas others are plant-specific, such as RSp31 (Lopato et al., 1996, 1999b, 2002; Lazar and Goodman, 2000; Gao et al., 2004; Isshiki et al., 2006). Recent studies have focused on the localization and dynamics of *Arabidopsis* SR splicing factors in plant cells using immunofluorescence microscopy and green fluorescent protein (GFP) translational fusion. Plant SR splicing factors localize into irregular nuclear domains frequently similar to mammalian speckles (Ali et al., 2003; Docquier et al., 2004; Fang et al., 2004; Lorkovic et al., 2004; Tillemans et al., 2005). Small clusters of interchromatin granules have also been described in differentiated *Arabidopsis* cells and have been shown to correspond to SR protein–containing speckles (Docquier et al., 2004; Fang et al., 2004). We previously evaluated an *Agrobacterium tumefaciens*–mediated transient expression assay to investigate SR protein dynamics in vivo and performed an analysis of SR protein colocalization using confocal microscopy (Tillemans et al., 2005). We showed that a distinct *Arabidopsis* SR protein, RSZp22, localizes in the nucleoplasm, in the nuclear speckles, and, intriguingly, also in the nucleoli, albeit at a lower level in physiological conditions. We also suggested that phosphorylation of the RS domain might influence its subnuclear localization. Interestingly, recent proteomic investigations of human and *Arabidopsis* nucleoli have identified many proteins involved in pre-mRNA metabolism, including SR splicing factors (Andersen et al., 2002; Scherl et al., 2002; Pendle et al., 2005). Based on these and additional data, it has been suggested that the nucleoli play a role in mRNA metabolism, including postsplicing events.

Understanding the cellular dynamic distribution of RSZp22 requires a more detailed knowledge of the functional domains of the protein implicated in its localization. To date, the dynamic properties of RSZp22 and other plant SR proteins in the nucleus and, more precisely, in the nucleolus have not been fully assessed using photobleaching techniques. To address these issues, we analyzed the subcellular localization of mutants and fragments of RSZp22 as fusion proteins with GFP in transiently expressing cells. We previously suggested the interest of transient transformation for such an approach (Tillemans et al., 2005). The structure of RSZp22, homologous with human SRp20 and 9G8, consists of an N-terminal RRM domain, followed by a Zn knuckle motif embedded in an RGG-rich region, and a C-terminal RS domain (Lopato et al., 1999a, 2002). Although the RGG motif is reminiscent of other described nucleolar localization signals, the localization of RSZp22 within the nucleolus may be associated with several functional mechanisms. We also investigated the intranuclear mobility of RSZp22-GFP using fluorescence recovery after photobleaching (FRAP) and fluorescence loss in photobleaching (FLIP) experiments and asked whether its mobility is dependent on ongoing transcription and/or the phosphorylation/dephosphorylation cycle. We show that this SR splicing factor shuttles rapidly between subnuclear compartments, including the nucleolus, and that inhibition of phosphorylation appears to influence its mobility.

Identifying plant shuttling SR proteins and understanding the nucleocytoplasmic transport mechanisms of these splicing regulators are of key importance with regard to their possible role in postsplicing events, such as mRNA export and/or nonsense-mediated decay. To address this question, we developed a sensitive shuttling assay based both on FLIP and on nuclear export inhibition after *Agrobacterium*-mediated transient expression. Using leptomycin B (LMB), a potent nuclear export inhibitor, we strongly suggest that RSZp22 is a nucleocytoplasmic shuttling SR splicing factor.

To gain insight into the dynamic organization of SR splicing factors in plants, we had previously generated transgenic *Arabidopsis* expressing GFP-tagged RSp31, a structural plant-specific SR protein. Cell type–dependent organization of RSp31 was observed in the primary root (Docquier et al., 2004). To test whether RSp31 can transiently associate and/or accumulate within the nucleolus in a cell type–dependent manner, inhibitions of transcriptional and kinase activities were performed. We discovered that inhibition of kinase activity led to a perinucleolar redistribution of RSp31 in all cell types, suggesting a higher order nuclear architecture in living plant cells.

Together, our findings provide new insights into nuclear organization in plants. Here, using photobleaching techniques, we show that RSZp22-GFP is highly mobile within the nucleus and in continuous flux between different nuclear compartments in vivo; also, its dynamics is dependent on the functional state of the cell. Our data demonstrate a link between the dynamics and localization of SR splicing factors and kinase activity, indicating that the phosphorylation-dependent redistribution and nucleolar capping of SR proteins may be an active and controlled process in the reorganization of nuclear compartments. Thus, the partitioning of *Arabidopsis* SR splicing factors supports a higher-order nuclear architecture in the plant interphase nucleus. Little is known about the regulation of nucleocytoplasmic shuttling of plant SR proteins. Additionally, we suggest that RSZp22, which is found in the nucleus at steady state, is a CRM1-dependent shuttling protein.

RESULTS

This study is based on the constitutive expression of fluorescent protein–tagged SR proteins after *Agrobacterium*-mediated transient transformation. We previously reported the use of transient transformation for the study of SR protein dynamic distribution and photobleaching experiments (Docquier et al., 2004; Tillemans et al., 2005). The fluorescence of fusion proteins reached a maximum at 2 d after agroinfiltration and gradually decreased over a period of several days, allowing the in vivo analysis of GFP fusion protein dynamics at different expression levels. Therefore, we analyzed cells characterized by different expression levels of fusion proteins and observed comparable localization and dynamics between them. Nevertheless, to avoid overexpression, cells with a medium to low expression of fluorescent protein–tagged

RSZp22 were preferentially selected for dynamic analysis and photobleaching experiments.

Nucleolar RSZp22 Targeting Is Mediated through Several Determinants

RSZp22 complements the splicing-deficient S100 cytosolic HeLa cell extract and therefore is likely to act as a splicing factor (Lopato et al., 1999a, 2002). In our previous report, we showed that RSZp22-GFP proteins display nucleoplasmic and nucleolar localization, with a higher concentration in speckle-like structures. In our transient expression assay and among the different SR proteins that we tested previously, RSZp22 was the only SR protein showing such a distribution. Its nucleolar localization was greatly enhanced upon phosphorylation inhibition by staurosporine and upon long observation periods, inducing what we previously defined as experimental stresses (ExS) in both tobacco (*Nicotiana tabacum*) and *Arabidopsis* cells (Figure 1; data not shown). We previously suggested that these ExS are linked to ATP depletion and/or cold temperature (Tillemans et al., 2005). Here, we investigated the possible causes of the relocalization of RSZp22 and observed initially that only ATP depletion could rapidly mimic such ExS-induced localization (cf. Figure 1 with Supplemental Figure 1 online). Cold shock did not appear to significantly alter RSZp22 distribution in transiently expressing cells (see Supplemental Figure 1 online). Next, possible changes in ATP level upon ExS were investigated by determination of cellular ATP in leaf fragments. Increasing observation times—and, as a result, ExS—led to a continuous decrease in cellular ATP levels, clearly demonstrating a link between ExS and ATP depletion (Figure 2C). Regardless of whether or not ATP depletion is the only factor involved, we took advantage of such a progressive redistribution of RSZp22-GFP in the following experiments to determine rapidly which domain of the protein promotes its nucleolar targeting and to what extent.

RSZp22 is characterized by a central Zn knuckle motif of the CCHC type (KCYECGEXGHFARECR) inserted into an RGG-rich region, both located between the RRM and RS domains (Figure 1A). The RRM and RGG domains, as well as the Zn knuckle motif, are all known to contribute to RNA binding. It has been shown that Arg- and Gly-rich sequences, like GRG and RGG, are enriched in the nucleolar proteome (Leung et al., 2003). To determine further the mechanism by which RSZp22 moves from the nucleoplasm to the nucleolus, we constructed a series of GFP-tagged mutant derivatives, which were transiently expressed in tobacco leaf cells (Figure 1). Different RSZp22 mutants were studied: proteins lacking the entire RRM domain (ΔRRM) or lacking the entire RGG motif including the Zn knuckle (ΔRGG/ΔZn), or an RSZp22 mutant in which amino acids 214 to 288 are deleted corresponding to the RGG but not the Zn knuckle (ΔRGG; Figure 1A). We also fused the entire RGG fragment or the entire RRM domain to GFP (Figure 1).

The distribution of the GFP-tagged RSZp22 mutant proteins ΔRGG and ΔRGG/ΔZn was similar to that of the wild-type RSZp22-GFP and was almost indistinguishable under experimental stress. The mutant proteins displayed an exclusive nuclear distribution, with a more diffuse nucleoplasmic distribution and accumulation in speckle-like structures, although not to the same extent as in the wild-type protein. Interestingly, deletion of the RGG domain, including or not the Zn knuckle motif, did not result in a loss of nucleolar accumulation under experimental stress, strongly suggesting that this domain is not the only determinant necessary for RSZp22 accumulation within the nucleolus (Figure 1B). A large perinucleolar space could be observed upon ExS, surrounded by numerous aggregates in the nucleoplasm. Next, the role of the RRM domain in subnuclear localization was determined. In unstressed cells, RSZp22ΔRRM was found to be exclusively nuclear, with a nucleoplasmic and speckled distribution. RSZp22ΔRRM showed the same predominant nucleolar localization as the full-length RSZp22 upon ExS (Figure 1B). The distribution of RSZp22 mutants in which the RS domain is deleted (ΔRS) has been described previously (Tillemans et al., 2005), and, as expected, RSZp22ΔRS was found to be distributed in the cytoplasm and the nucleus. The deletion of the RS domain induced an immediate nucleolar localization of the mutants (Figure 1B).

Next, the RGG domain including the Zn knuckle motif was fused to GFP and was transiently expressed. Interestingly, confocal imaging showed a cytoplasmic and homogeneous nuclear localization and a distribution of the chimeric protein in the nucleoplasm and slightly in the nucleoli (Figure 1B). After 2 h of observation, RGG-GFP was present but was not concentrated in the nucleolus. After a longer period of observation, RGG-GFP increased slightly within the nucleoli. Although this result suggests its role in nucleolar targeting, it clearly shows that RGG is not the only motif responsible for nucleolar RSZp22 localization. Finally, RRM-GFP was also observed in both the nucleus and the cytoplasm but was excluded from the nucleoli in normal conditions (Figure 1B). Only extensive ExS (and, therefore, ATP depletion) promoted an increase in RRM-GFP nucleolar localization, albeit to a lesser extent than for RGG-GFP.

The RGG motif, including or not the Zn knuckle, does not seem to be required in its complete form for nucleolar targeting, because we found that the expression of RSZp22 lacking in this sequence resulted in nucleolar distribution upon ExS (including ATP depletion). Together, our results suggest that the nucleolar localization of RSZp22 might be a consequence of the interactions of its diverse domains with nuclear and/or nucleolar factors, possibly through RNA binding and/or protein–protein interactions, and is not attributable to one unique nucleolar localization signal.

RSZp22 Shuttles Rapidly between Subnuclear Compartments, and Its Mobility Is Dependent on Kinase Activity

To date, the dynamic properties of RSZp22-GFP in the nucleus and between nuclear compartments have not been addressed. Having established that RSZp22-GFP is localized and/or accumulated in response to specific stresses in the nucleolus, we wished to determine whether this compartmentalization is dynamic. Therefore, we conducted photobleaching experiments using time-lapse confocal microscopy.

We first addressed the dynamics of RSZp22-GFP using FRAP (Figure 2; see Supplemental Movie 1 online). GFP fluorescence was irreversibly bleached in small circular areas of the

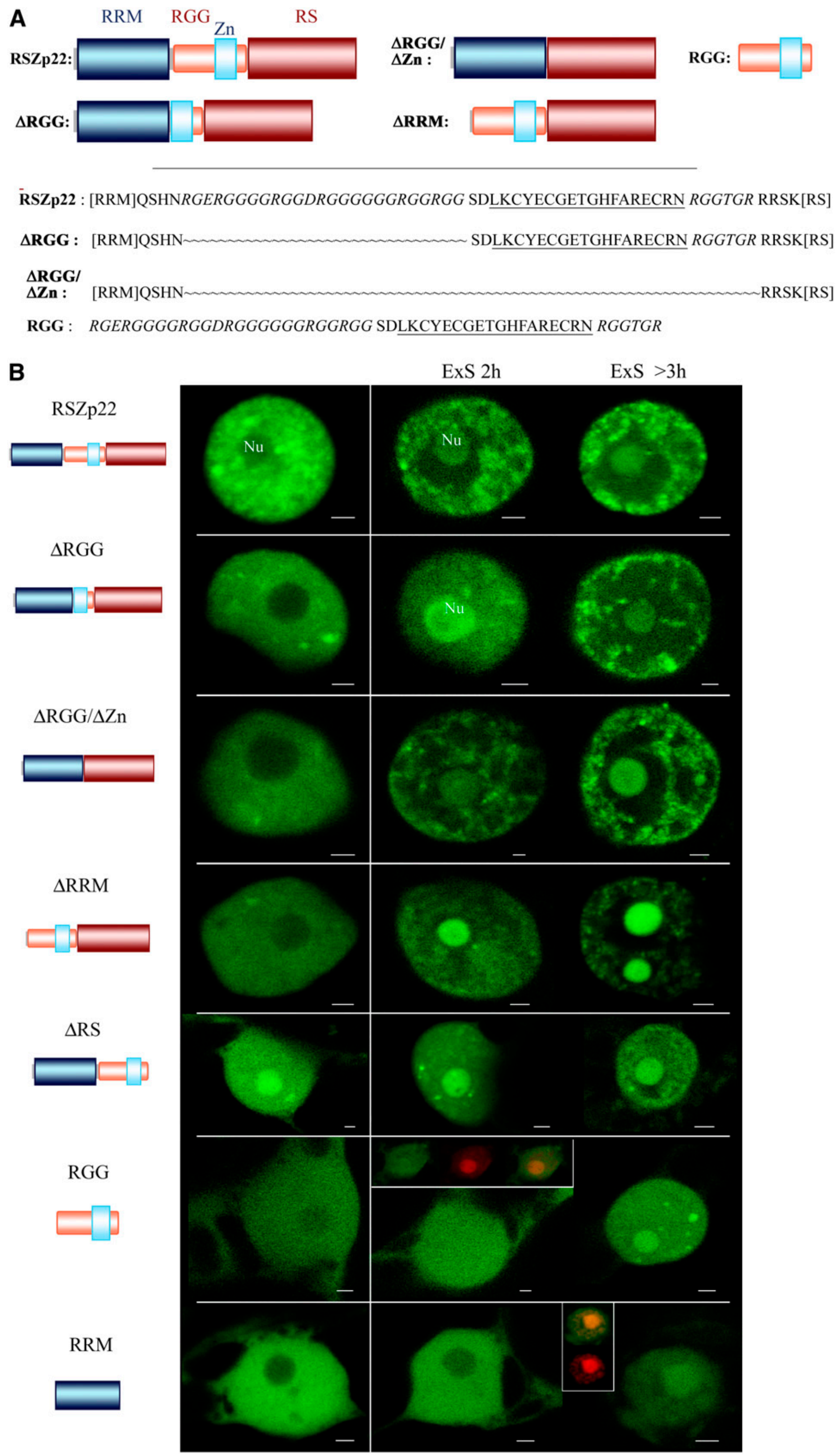

Figure 1. RSZp22 Structural Domains and Localization of Wild-Type and RSZp22 Mutant Proteins in Interphase Nuclei.

nucleoplasmic pool, in the speckles, or in the nucleolus. The fluorescence recovery was then monitored over time within this specific region by sequential imaging. As shown in Figure 2, the fluorescence recovered rapidly after photobleaching within the nucleoplasm, speckles, and nucleoli. In our experiments, RSZp22-GFP recovered to 90 to 100% over the course of 3 to 4 s, with a half-time of recovery of ~0.4 to 0.5 s in all nuclear compartments. These data are not in the same range as our previously reported values for other SR proteins; this discrepancy can be explained by the use here of the Fly-mode for FRAP (Leica MicroLab module), which allows analysis of very fast recovery kinetics (see Methods). We ensured that bleaching did not cause damage to the cell by performing consecutive FRAP experiments within the same nuclear territory. These each displayed similar fluorescence recovery kinetics.

We previously showed that inhibition of transcription and (de)phosphorylation induced *Arabidopsis* SR proteins to be redistributed in larger nucleoplasmic regions concomitant with the disappearance of the diffuse fraction (Tillemans et al., 2005). We also asked whether altering the (de)phosphorylation process or the transcriptional activity had an effect on the dynamics of RSZp22-GFP. Leaf cells were incubated with staurosporine (a general inhibitor of protein kinases) or okadaic acid (an inhibitor of phosphatases). Although we are conscious that these drugs block the overall cellular phosphorylation/dephosphorylation cycle, they have been—and still are—used extensively to investigate whether changes in the phosphorylation state of proteins are responsible for altering their activity and/or their dynamics within cells (Misteli et al., 1997; Kruhlak et al., 2000; Weingartner et al., 2001; Ali et al., 2003; Liu et al., 2005a, 2005b). Upon okadaic acid treatment, RSZp22-GFP mobility was decreased slightly, with a half-time of recovery ranging from 0.6 to 1.2 s. Treatment by α-amanitin, a potent inhibitor of RNA polymerase II transcription, also slightly decreased the fluorescence recovery, mainly within the speckles. Strikingly, upon staurosporine treatment, we observed that large nucleoplasmic speckle-like structures were noticeably static, with no or weak fluorescence recovery after photobleaching (Figure 2B). Regardless of whether this is a direct or indirect effect of the inhibitor, this observation indicates that kinase activity is required for the rapid RSZp22 dynamics within both the nucleoplasm/speckles and the nucleoli. Furthermore, during the process of ExS inducing progressive ATP depletion, the mobility of RSZp22-GFP was affected in a proportional manner to the level of stress that the cells experienced (Figure 2C). Drug-induced ATP depletion abolished RSZp22-GFP dynamics (see Supplemental Figure 1 online). Although these data suggest that the association and dynamics of RSZp22 within the nucleoli might be energy-dependent, we consider the possibility that ATP depletion also alters other cellular events, including the phosphorylation state of proteins.

RSZp22-GFP FRAP experiments in the nucleoplasm and nucleoli suggest rapid cycling of the protein between these nuclear compartments. To test this question further, we performed a FLIP analysis (Figure 3). The FLIP analysis consisted of repeatedly bleaching a region of interest within either the nucleoplasm or the nucleolus while sequentially imaging the nucleus at regular intervals (see Methods). When a region of the nucleoplasm was bleached repeatedly, RSZp22-GFP fluorescence decreased gradually over the overall nucleus, including the nucleoli. Similar data were obtained by bleaching a region within the nucleolus (Figure 3).

Together, these data confirm that RSZp22 cycles rapidly and continuously between the nucleoplasm and the nucleolus in a phosphorylation- and ATP-dependent manner.

RSZp22 Is a Nucleocytoplasmic Shuttling Protein

Because it is known that FLIP experiments can address the question of whether a protein shuttles across a cellular compartment (Lippincott-Schwartz et al., 2001), we developed a FLIP-based assay in leaf cells after transient transformation. We repeatedly bleached a region of the cytoplasm surrounding the nuclei and investigated the fluorescence level of RSZp22-GFP within them (Figure 4; see Supplemental Movies 2 and 3 online). It should be noted that shuttling SR proteins are localized in the nuclei at a steady state. If RSZp22 is not a nucleocytoplasmic shuttling protein, the fluorescence of RSZp22-GFP should remain constant during all of the FLIP experiments involving the repeated bleaching of the cytoplasm. On the other hand, if RSZp22 shuttles rapidly between the nucleus and the cytoplasm, the fluorescence of the fusion proteins should decrease continuously during FLIP. To determine whether RSZp22 is a nucleocytoplasmic shuttling protein, we evaluated FLIP after *Agrobacterium*-mediated transient expression. To substantiate this approach, we combined FLIP with LMB inhibition. Proteins exported from the nucleus often possess a distinct, Leu-rich nuclear export signal (or NES), which can form a ternary complex with an export receptor, termed CRM1/exportin1 (also termed XPO1/exportin1). LMB has been described as specifically inhibiting NES-mediated export by interacting with CRM1/exportin1. It has been shown that *Arabidopsis* CRM1/exportin1 contains the Cys residue that is alkylated by LMB and that plant cells are indeed sensitive to this inhibitor (Igarashi et al., 2001). If RSZp22 shuttles between the nucleus and the cytoplasm, the

Figure 1. (continued).

(A) Scheme of the structural domains of RSZp22 and of the mutant derivatives generated. Details of the wild-type sequence and of internal deletion of the RGG/Zn knuckle domain are shown. The RGG is shown in italics, and the Zn knuckle is underlined.

(B) Confocal microscopy of nuclei expressing RSZp22-GFP and the GFP-tagged mutant proteins in physiological conditions and upon ExS (see text for details). Nu, nucleolus. Cells expressing RGG or RRM fused to GFP were counterstained for nucleic acid detection to facilitate nucleoli localization (in the insets, red fluorescence marks the nucleoli), and merging of the two areas of fluorescence shows the nucleolar localization of both RGG- and RRM-GFP upon ExS. Bars = 2 μm.

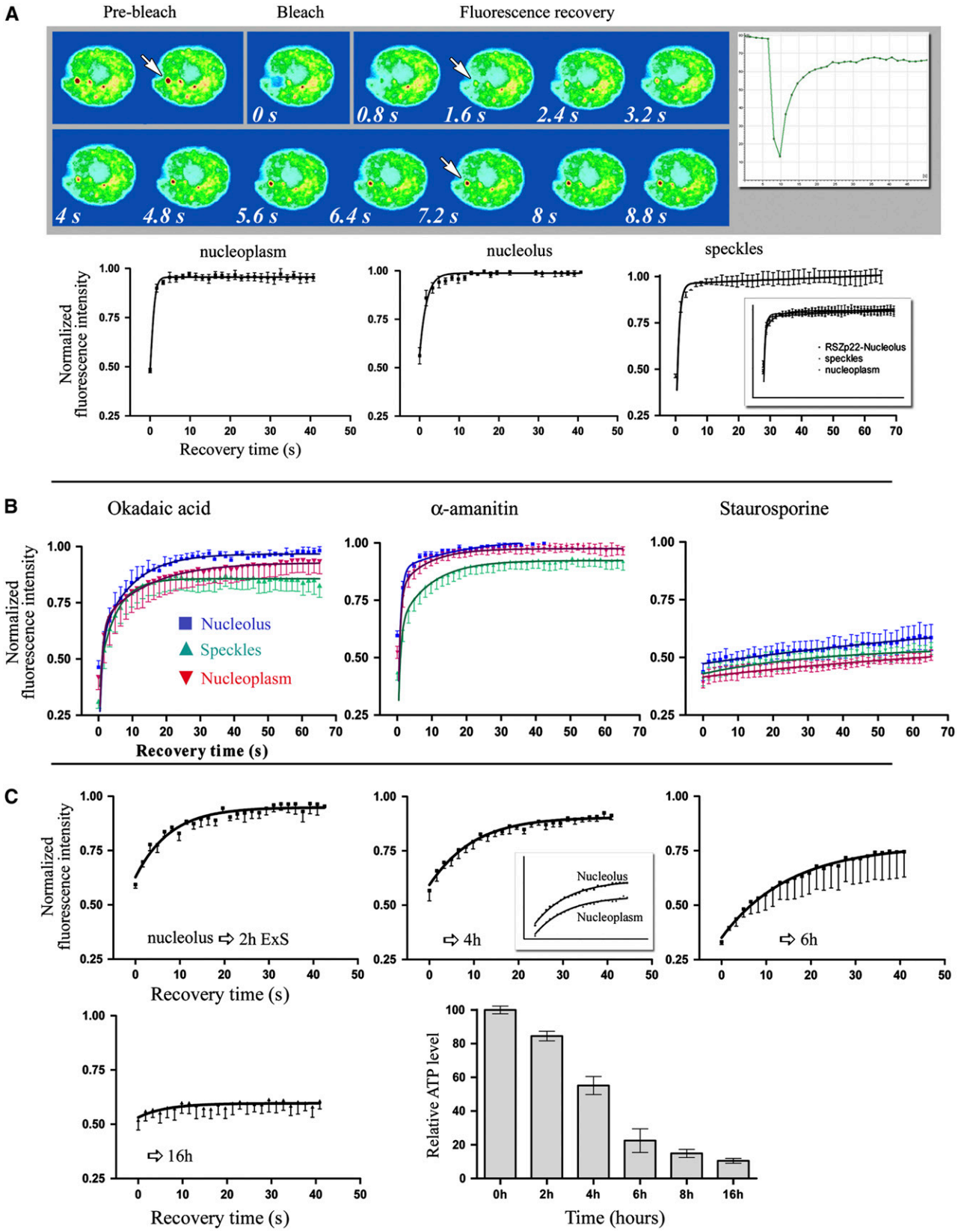

Figure 2. RSZp22 Is Highly Dynamic within the Nucleus and Associates with the Nucleolus.

RSZp22-GFP fluorescence should remain constant in the nucleus upon treatment with LMB.

As shown in Figure 4 and in Supplemental Movie 2 online, RSZp22-GFP fluorescence in the nuclei was strongly reduced during the course of cytoplasmic photobleaching, suggesting that RSZp22 shuttles between the nucleus and the cytoplasm. FLIP experiments on leaf cells treated with LMB noticeably revealed the absence of a decrease in fluorescence in the nucleus, indicating that LMB blocks the export mechanism of RSZp22-GFP (Figure 4; see Supplemental Movie 3 online). Short LMB treatments resulted in a nucleolar localization of RSZp22-GFP, and, strikingly, longer treatments led to a significant accumulation of RSZp22-GFP in internal nucleolar components (Figure 5A; see Supplemental Movie 4 online). As revealed using FRAP, LMB treatment did not result in a severe loss of RSZp22 mobility within the nucleolus compared with ATP depletion and staurosporine treatment, which also resulted in RSZp22 nucleolar accumulation (cf. Supplemental Figure 1 online and Figures 2B and 2C with Figure 5B). Moreover, to further validate this approach, we performed the FLIP-based assay on both (1) the GFP-fused tomato (*Lycopersicum peruvanium*) heat stress transcription factor HsfA1, which is a shuttling protein with an NES-like motif at its C terminus, and (2) the reporter constructs GFP-NLS-CHS-NES_{Rev} and GFP-NLS-CHS-$NES(-)_{Rev}$, which consist of the GFP fused to chalcone synthase bearing an active nuclear localization signal (NLS) and an active NES and a mutated inactive NES, respectively (Haasen et al., 1999; Heerklotz et al., 2001). As shown in Supplemental Figure 2 online, the relative nuclear fluorescence of HsfA1-GFP and GFP-NLS-CHS-NES_{Rev} decreased exponentially during the FLIP experiment. LMB treatment resulted in the absence of a decrease in fluorescence of HsfA1-GFP and GFP-NLS-CHS-NES_{Rev}, similar to that observed with RSZp22. As expected, the fluorescence of GFP-NLS-CHS-$NES(-)_{Rev}$ remained constant or even increased slightly during the FLIP time lapse (see Supplemental Figure 2B online). Thus, although LMB has not been used widely in plant systems to date, we suggest that it could provide an efficient control in the process of understanding the nucleocytoplasmic shuttling of SR proteins in plant cells.

Next, we asked whether RSZp22-GFP nucleocytoplasmic shuttling is influenced by cellular phosphorylation activity and ATP level. Both staurosporine and ATP depletion were shown to block the export of RSZp22-GFP (Figures 6A and 6B), suggesting that the absence of RSZp22 mobility upon these drug treatments might also be an indirect consequence of a general freezing of the nuclear molecules.

To investigate whether the RGG and/or the Zn knuckle motifs promote RSZp22 nuclear export, FLIP shuttling experiments were performed within cells expressing GFP-tagged RSZp22ΔRGG or RSZp22ΔRGG/ΔZn. Intriguingly, opposite to the full-size proteins, deletion of both the RGG motif and the RGG/Zn knuckle domain provided variable results with regard to export properties (Figures 6C and 6D). We observed different kinetics of loss of fluorescence using the FLIP shuttling assay, mainly on RSZp22ΔRGG/ΔZn. In many cells, the decrease in fluorescence was similar to that described for the full-size RSZp22-GFP, whereas in other cells, it was less severe. Although this variability in loss of fluorescence suggests a possible role of the RGG/Zn knuckle domain in the export event, it is not clear at this point why the shuttling of RSZp22-deleted mutants may vary depending on the individual cell selected for analysis. With the nuclear localization signals being present in the RS domain, the FLIP shuttling experiment could not be tested in RSZp22ΔRS mutant proteins.

RSp31 Is Not Nucleolar but Is Redistributed within the Nucleolar Caps

In transiently expressing leaf cells, RSZp22 was the only SR protein among several that was dynamically (re)distributed within the nucleolar territory. We were interested in investigating whether another SR protein could associate at least transiently with the nucleolus in a cell type–dependent manner. We used *Arabidopsis* transgenics expressing RSp31-GFP, which we had generated previously (Docquier et al., 2004), and seedlings were treated with okadaic acid, staurosporine, α-amanitin, or with water as a control (Figure 7). After okadaic acid and α-amanitin treatments, RSp31-GFP from root cells accumulated into static large speckles. Strikingly, staurosporine treatment led to a severe accumulation of fusion proteins into concave cap-like structures surrounding regions devoid of fluorescence, corresponding to the nucleoli. Staurosporine promoted such a redistribution in all cell types of the primary root, from meristematic cells to (a)trichoblasts (Figure 7A). We observed a similar RSp31

Figure 2. (continued).

(A) FRAP analysis of RSZp22-GFP in transiently expressing cells. A region of interest within the nucleus (indicated by arrows) was photobleached, and the fluorescence recovery was monitored at regular intervals (every 0.8 s after bleaching). The noncorrected recovery curve of this specific nucleus is shown (top right). The series of selected confocal images shows the fluorescence recovery in one bleached speckle. The recovery of fluorescence was monitored and averaged for several independent experiments within the nucleoplasmic pool (left graph), nucleolus (middle graph), or speckles (right graph). One hundred percent fluorescence indicates the prebleach fluorescence intensity. The inset in the right graph shows the three recovery curves on the same graph (error bars indicate SE).

(B) Effect of the inhibition of (de)phosphorylation and transcription on RSZp22 mobility. Cells transiently expressing RSZp22-GFP were photobleached, and fluorescence recovery is shown within the nucleoplasm, speckles, and nucleolus after drug treatment with okadaic acid (left), α-amanitin (middle), and staurosporine (right).

(C) RSZp22 mobility decreases upon ExS, inducing ATP depletion. Small circular regions within nucleoli were photobleached in cells that experienced ExS for different lengths of time, from 2 to 16 h. Recovery kinetics in the nucleoplasm and in the nucleoli were similar, as shown in the middle graph, after 4 h of ExS. The histogram (bottom right) shows the effects of ExS on cellular ATP levels. The time is measured from the time of cutting and placing leaf fragments between slides and cover slips. The average value calculated for time 0 was set as 100%, and the values obtained at different times were expressed relative to this value. All values are means ± SE ($n = 6$).

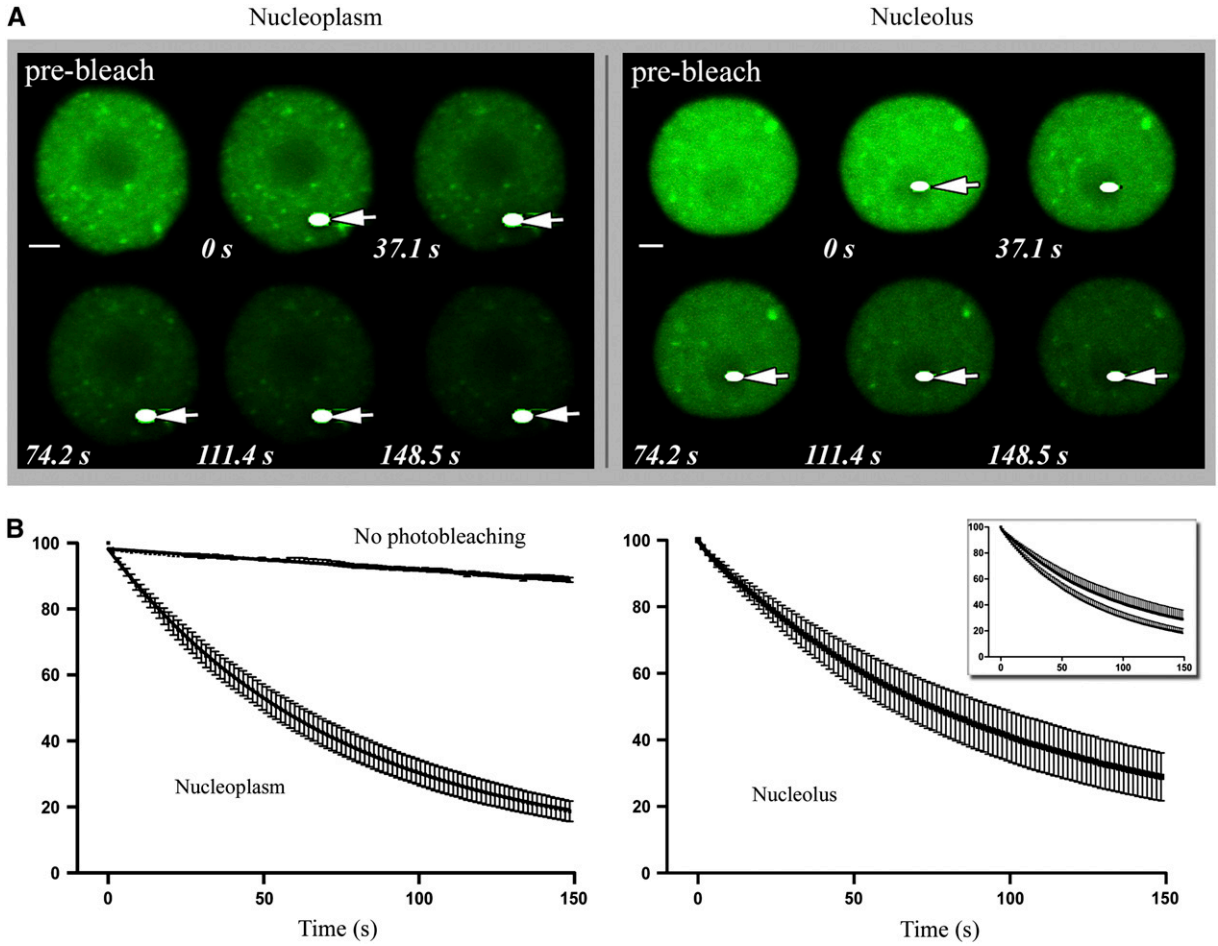

Figure 3. Loss of Fluorescence in Photobleaching Analysis of RSZp22-GFP.

(A) Selection of confocal images of nuclei of transiently expressing cells during FLIP experiments. The arrows show the bleached areas (white dots) that were selected within the nucleoplasm (left) or the nucleolus (right). Time (expressed in seconds) is indicated at bottom of each frame.
(B) Quantitative FLIP. Bleached areas were chosen within the nucleoplasm or the nucleolus. Both graphs are represented in the inset. One hundred percent indicates the prebleach nuclear fluorescence intensity (error bars indicate SE). As a control, nuclei expressing RSZp22-GFP were repeatedly scanned under normal (nonphotobleaching) conditions, and the slight decrease of fluorescence was quantified.

redistribution in transiently expressing *Arabidopsis* leaf cells (Figure 7B). The perinucleolar localization of RSp31 proteins was shown to be reversible, because the RSp31-GFP relocalized into nucleoplasmic speckles upon the return to physiological conditions. We ensured that seedlings were still viable after drug treatments. Okadaic acid and α-amanitin treatments did not result in RSp31 accumulation around the nucleolus (Figures 7A and 7B). To learn about the RSp31 redistribution at the ultrastructural level, electron microscopy was performed on staurosporine-treated seedlings. As shown in Figure 7C, fibrillar and granular materials were observed surrounding the electron-dense nucleoli. Comparing the results of the fluorescent distribution of RSp31-GFP with the electron micrographs, the materials observed around the nucleolus could correspond to RSp31-containing nucleolar caps. No such perinucleolar fibrillar or granular materials were observed in control cell seedlings (Figure 7C). Interestingly, cap-like structures are reminiscent of other perinucleolar components that have been described in animal cells under transcriptional arrest (Shav-Tal et al., 2005). It has been shown that nucleoplasmic RNA binding proteins, and not only nucleolar factors, are redistributed from the nucleoplasm to specific nucleolar caps (Shav-Tal et al., 2005).

DISCUSSION

One characteristic of eukaryotic cell nuclei is the presence of dynamic nuclear compartments, which has been linked to nuclear and cellular processes, including chromatin remodeling, regulation of gene expression, ribosome biogenesis, splicing, post-splicing events, and cell cycle–associated mechanisms (Dundr and Misteli, 2001; Yanovsky et al., 2002; Lamond and Spector, 2003; Bernardi et al., 2004; Moriguchi et al., 2005; Zemach et al., 2006). Nowadays, the functional architecture of the nucleus has to be thought of as a dynamic steady state rather than as a static

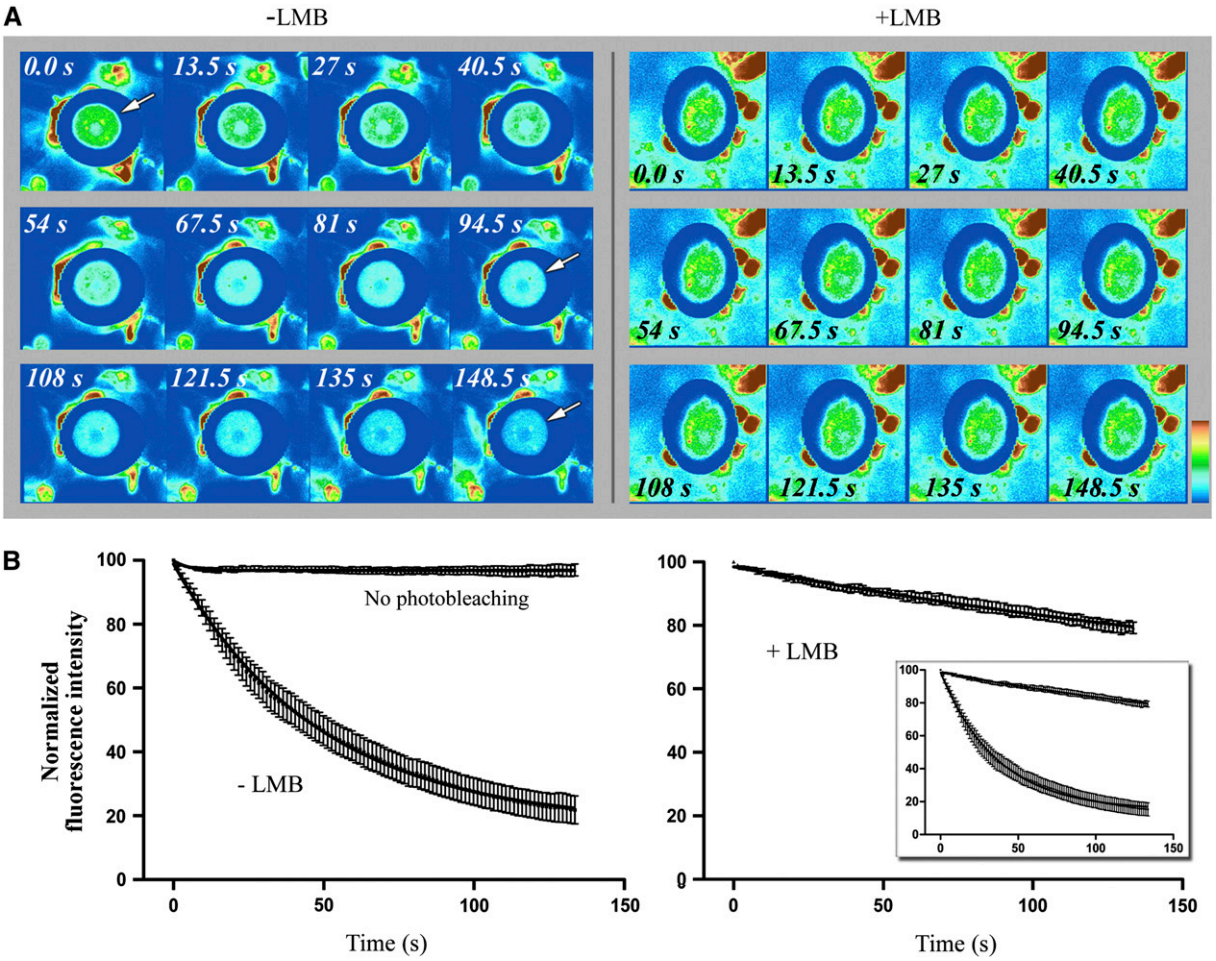

Figure 4. Sensitive FLIP-Based Nucleocytoplasmic Shuttling Assay of RSZp22.

(A) FLIP in transiently RSZp22-expressing living cells without (left; −LMB) or with (right; +LMB) LMB treatment. A large cytoplasmic area was repeatedly bleached, and the loss of fluorescence within the nucleus was measured over time. The selection of serial optical sections shows loss of fluorescence in the overall surface of the nucleus; the arrow points to the nucleus. Upon LMB treatment, qualitative observations did not reveal significant loss of fluorescence within the nucleus over time.

(B) FLIP quantification. The loss of fluorescence was monitored and averaged, and the curves clearly show that LMB treatment blocks nucleocytoplasmic shuttling of RSZp22. As an additional control, cells expressing RSZp22-GFP were repeatedly scanned under nonphotobleaching conditions, and the slight decrease of nuclear fluorescence was quantified. One hundred percent fluorescence indicates prebleach fluorescence intensity. The insert shows curves from untreated and LMB-treated cells on the same graph.

situation. In metazoans, several studies using photobleaching techniques have established the dynamic properties of SR splicing factors (Kruhlak et al., 2000; Phair and Misteli, 2000). Plant nuclear organization and dynamics remain comparatively poorly understood. Here, we demonstrate that the *Agrobacterium*-mediated transient expression assay combined with photobleaching experiments can be used effectively to report on SR protein dynamics and their nucleocytoplasmic shuttling.

Distribution of the RSZp22 SR Protein Depends on Several Determinants

The subnuclear distribution of proteins either depends on direct targeting attributable to internal signal sequences or is established through interactions with binding partners. To date, it has been difficult to identify canonical/consensus sequences that target all nuclear proteins to the many different subnuclear compartments, including the nucleolus (Leung et al., 2003). To define the sequence requirements for RSZp22 localization, we undertook a mutational analysis of the protein and generated fluorescent protein–tagged deletion mutants. Wild-type RSZp22 displays a predominant nuclear speckled organization. Here, we show that not only the RS but also the RRM and RGG domains of RSZp22 are involved in speckled patterns, indicating that the integrity of the protein is essential for its distribution. In addition to its concentration in speckles, RSZp22 is also localized in the nucleolus at low levels in physiological conditions (Tillemans et al., 2005; this report). Only the deletion of the RS domain

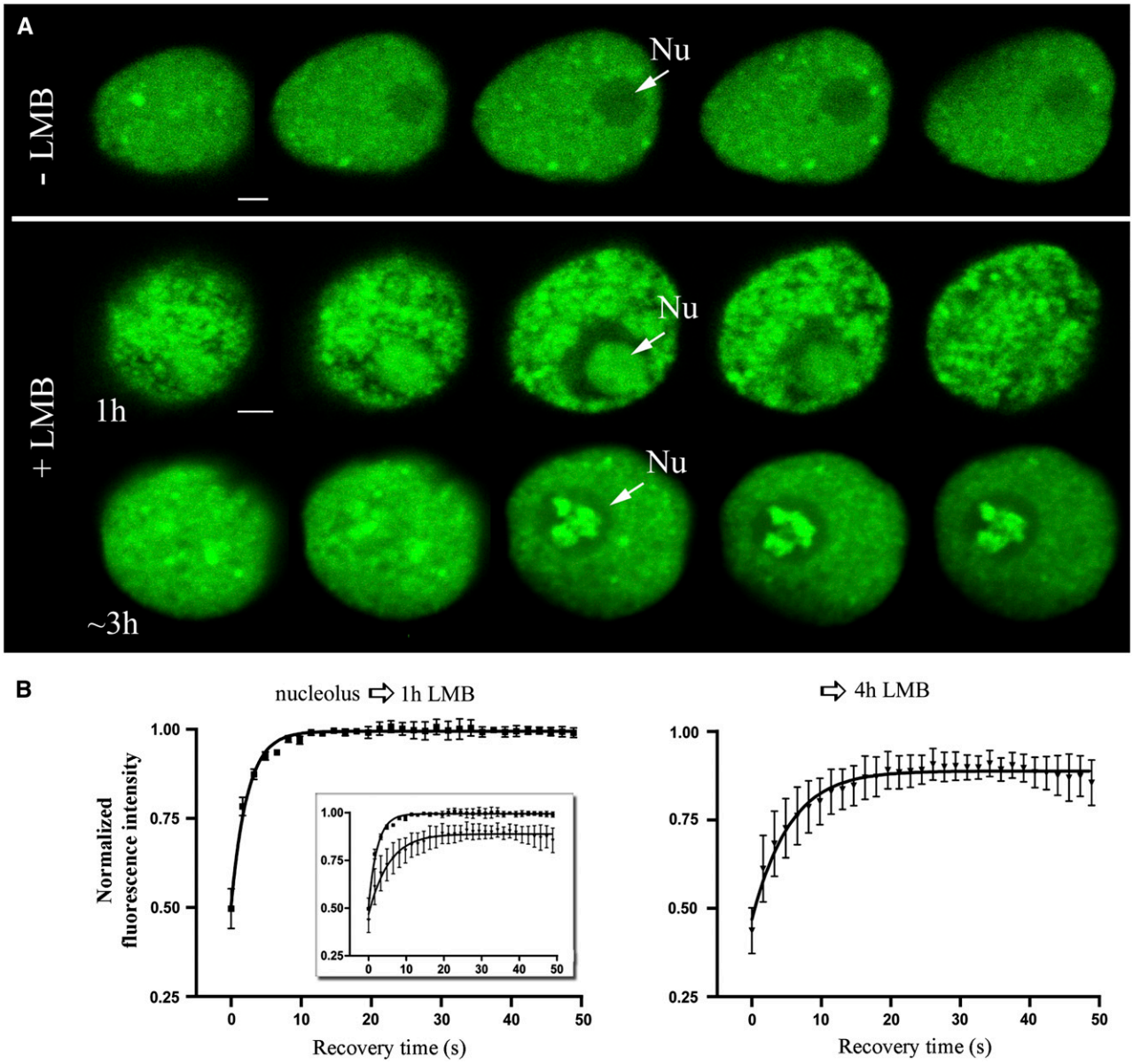

Figure 5. Nuclear Localization and Dynamics of RSZp22 upon LMB Treatment.

(A) RSZp22-GFP subnuclear distribution in cells treated with water (as a control; top row) or LMB (middle and bottom rows). The selection of serial optical sections through the nuclei shows a homogeneous RSZp22 distribution within the nucleolus after an LMB treatment of 1 h (middle row) and its concentration in intranucleolar domains (arrows) after a treatment of ~3 h (bottom row). Nu, nucleolus. Bar = 2 μm.

(B) LMB treatment does not severely affect the mobility of RSZp22 within the nucleoli, as shown by the kinetics of the fluorescence recovery after photobleaching. One hundred percent fluorescence indicates prebleach fluorescence intensity. The insert shows the two curves in a single graph.

results in an immediate nucleolar accumulation independent of stresses that cells may experience. The other deletion derivatives, ΔRRM, ΔRGG, and ΔRGG/ΔZn knuckle, localize to the nucleolus upon experimental stresses that induce progressive and continuous ATP depletion. So, how does the deletion of the RS domain lead to nucleolar accumulation?

One explanation would be that the RS domain of the wild-type protein interacts with binding partners in the nucleoplasm and the speckles and keeps RSZp22 out of the nucleolar territory. However, human SR proteins and RSp31 with their RS domain deleted have been shown not to display nucleolar redistribution, suggesting that an additional signal along the RSZp22 sequence may be required for nucleolar targeting (Caceres et al., 1997; Misteli et al., 1998; Tillemans et al., 2005). By definition, a sequence targeting signal corresponds to a protein motif that is necessary and sufficient for subcellular distribution independently

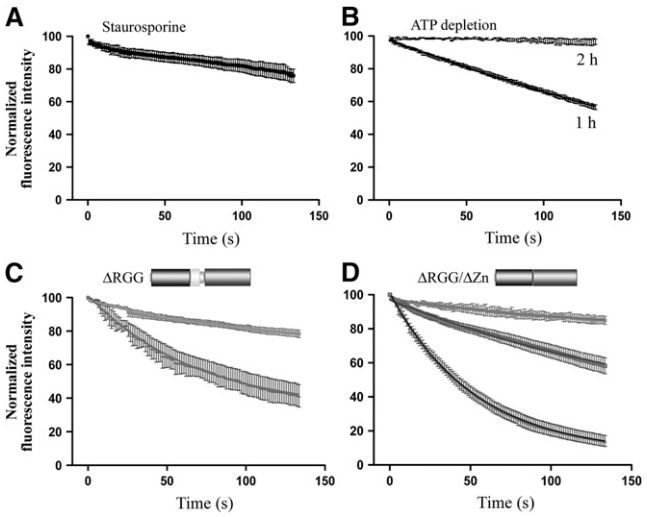

Figure 6. Effect of Phosphorylation Inhibition and ATP Depletion on the Nuclear Export of RSZp22, and Role of the RGG Domain in Its Nucleocytoplasmic Shuttling.

(A) and **(B)** FLIP experiments show that nucleocytoplasmic shuttling of RSZp22 depends on the phosphorylation state of the cell **(A)** and on ATP depletion **(B)**. The curves show the kinetics of loss of fluorescence within the nuclei.

(C) Role of the RGG domain in the nuclear export of RSZp22. The graph shows different kinetics of fluorescence intensity decrease within the nuclei, from a weak level to a fluorescence intensity decrease similar to that of the full-size protein.

(D) The nuclear export of RSZp22 is altered when the RGG domain and the Zn knuckle are deleted. The graph shows three different kinetics of fluorescence intensity decrease within the nuclei.

of its position and that therefore can target chimeric proteins to this specific localization. The nucleolus is known to be the seat of ribosome biogenesis, and nucleolar-resident proteins often contain Arg-, Lys- and/or Gly-rich motifs (Leung et al., 2003; Angelier et al., 2005; Pendle et al., 2005; Thiry and Lafontaine, 2005). The RGG domain of Ma16 (Gendra et al., 2004) or *Arabidopsis* fibrillarin (Pih et al., 2000) is involved in nucleolar targeting, and it has been shown that the C-terminal RGG domain of nucleolin is responsible for the interaction with distinct ribosomal proteins (Bouvet et al., 1998). Thus, the RSZp22 RGG motif is reminiscent of described nucleolar localization signals. Yet, we show that the RSZp22 RGG motif alone is not sufficient to concentrate RGG-GFP to the nucleolus in physiological conditions, demonstrating that it does not act as a (strong) nucleolar localization signal. Internal deletion of the RGG confirmed this, because deletion mutant proteins still display nucleolar localization upon experimental stress. Even though the RGG motif does not appear to act as a strong nucleolar targeting signal, it can contribute to RSZp22 internal concentration within the nucleolus upon LMB treatment.

For some proteins, nucleolar localization signals are instead considered as nucleolar retention signals, which generally consist of sequences rich in Arg and Lys, often overlapping nuclear localization signals (Catez et al., 2002). However, putative nuclear localization signals along the RSZp22 sequence are likely to be located in the RS domain (Tillemans et al., 2005). RSZp22ΔRRM mutant proteins are still concentrated in the nucleolus upon ExS, indicating that RRM-mediated binding to RNA is not required for nucleolar entry. Nor does the RRM domain act as a targeting signal. The nucleolar targeting process of the protein NO38 depends on the presence of two independent domains located at both the N- and C-terminal ends of the protein (Zirwes et al., 1997). It has been shown that the Gly/Arg-rich domain of nucleolin acts in synergy with at least one RRM domain for its total nucleolar accumulation, indicating the need for several determinants (Creancier et al., 1993). Therefore, we can assume that the RSZp22 nucleolar targeting most likely involves more complex signals/interactions than a simple sequence motif, although the RGG motif clearly participates in this targeting.

Nucleocytoplasmic Shuttling of SR Proteins

It has been proposed that the human shuttling SR proteins have to play multiple novel roles in postsplicing events (Huang and Steitz, 2005; Sanford et al., 2005). Despite their continuous shuttling, SR proteins are localized in nuclei at a steady state, and identifying them requires efficient and sensitive assays. An interspecies heterokaryon-based assay has been used to characterize animal nucleocytoplasmic shuttling SR proteins (Caceres et al., 1998). By contrast, little is known about the molecular mechanisms underlying nuclear shuttling in plant cells, in particular nuclear export (Haasen et al., 1999; Ward and Lazarowitz, 1999). In this study, we adopt three specific approaches for studying the shuttling of SR splicing factors. We combine *Agrobacterium*-mediated transient expression, photobleaching confocal microscopy, and nuclear export inhibition by LMB to investigate the nucleocytoplasmic shuttling of RSZp22. LMB inhibits the interaction of the karyopherin receptor CRM1/exportin1 with NESs (Haasen et al., 1999; Igarashi et al., 2001). Our findings suggest that RSZp22 shuttling is mediated by this export pathway. A closer look at the RSZp22 primary sequence did not reveal Leu-rich NES-like motifs (http://www.cbs.dtu.dk/services/NetNES/), indicating either that a weak NES-like motif remains to be discovered along the RSZp22 sequence or that CRM1-mediated RSZp22 export could be indirect, tethered to other molecules. We cannot exclude the possibility that nuclear export of RSZp22 proceeds by different coexisting mechanisms.

By swapping the corresponding domains between shuttling and nonshuttling human SR proteins, it has been shown that the RS domain is required for shuttling. However, the RS domain is not sufficient for shuttling; RNA binding through the RRM is also important (Caceres et al., 1998). Mutations altering the RNA binding capacity of RSZp22 should better define the function of the RRM domain in the shuttling process. Kinase inhibition by staurosporine also blocks RSZp22 shuttling, but this may reflect an indirect effect of the inhibitor. Indeed, CRM1/exportin1-mediated export also might be regulated by phosphorylation. Interestingly, RSZp22 proteins accumulate in the nucleolus upon longer LMB treatment. This striking accumulation could be attributable either to an increase in nucleolar targeting of the nucleoplasmic pool that cannot be exported to the cytoplasm or to prolonged nucleolar retention of a fraction that is normally exported, or both. Different kinetics of the loss of fluorescence

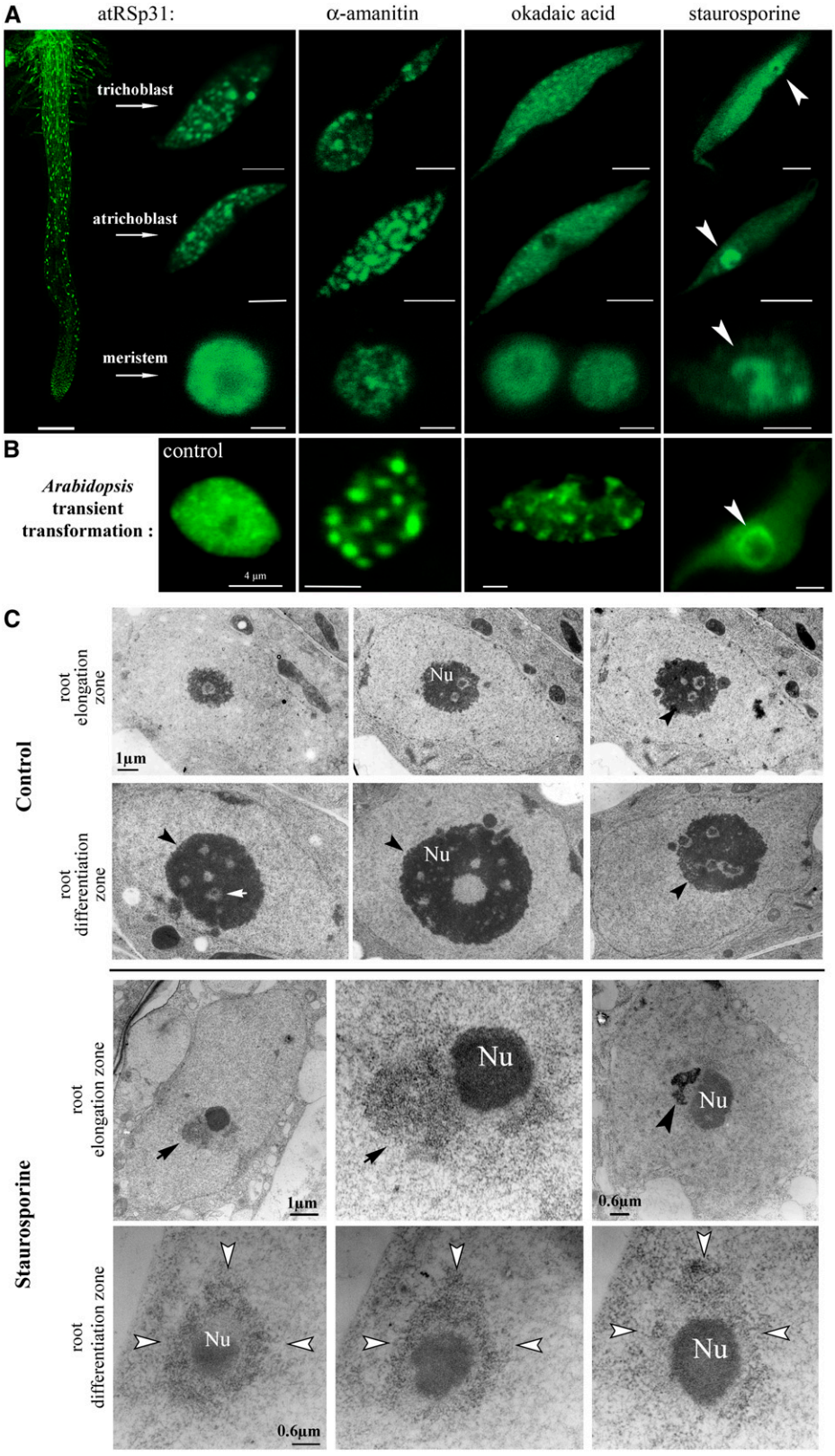

Figure 7. Effects of Inhibitor Treatments on the Subnuclear Organization of RSp31.

using the FLIP shuttling assay were readily apparent among cells expressing GFP-tagged RSZp22ΔRGG or RSZp22ΔRGG/ΔZn, in contrast with full-size RSZp22-GFP. Although these findings suggest a possible role of the RGG/Zn knuckle in the export process, we wish to stress that caution should be exercised when studying the dynamics of deleted protein. Knowing which SR protein shuttles is a first step toward understanding the regulation of the nucleocytoplasmic transport of SR splicing factors.

Nuclear Functional Dynamics of *Arabidopsis* SR Proteins

The nucleolus appears to be a very dynamic nuclear territory, with pre-rRNA processing factors exchanging very rapidly with the surrounding nucleoplasm (Phair and Misteli, 2000; Chen and Huang, 2001). It was previously unclear whether the RSZp22 splicing factor resides statically in the nucleolus or whether it shuttles continuously with the surrounding nucleoplasm. We attempted to address this question using photobleaching techniques that provide novel insights into the nature of RSZp22 dynamics. RSZp22-GFP moves rapidly in continuous flux between all nuclear compartments, including the nucleolus. Because a role for RSZp22 in pre-mRNA splicing seems highly probable (Lopato et al., 1999a), the question of the functional consequences of its unrestricted mobility between nuclear compartments remains. It recently became apparent that the nucleolus is a plurifunctional nuclear domain (Pederson, 1998; Politz et al., 2000; Pendle et al., 2005; Tsai and McKay, 2005). The nucleolar proteome contains an impressive number of proteins that have no apparent function in ribosome biogenesis, such as proteins related to ubiquitylation, RNA editing, signal recognition particle assembly, and (pre-)mRNA metabolism (Andersen et al., 2002; Scherl et al., 2002; Sansam et al., 2003; Azzam et al., 2004; van den Boom et al., 2004; Mekhail et al., 2005; Zemach et al., 2006).

Nucleolar proteomic analyses have been performed on both human and *Arabidopsis* nucleoli. In human, ~12% of the identified proteins are involved in the regulation of every step of mRNA metabolism, including SR splicing factors such as the Zn knuckle containing 9G8 (Andersen et al., 2002; Scherl et al., 2002). Those authors did not exclude the possibility that these proteins were found in small amounts and very transiently within nucleoli, rendering them difficult to visualize using other techniques such as immunolocalization. Therefore, GFP translational fusion eventually combined with confocal microscopy can be considered an extremely powerful approach to investigate the (dynamic) distribution of SR proteins. Recently, the profile of the *Arabidopsis* nucleolar proteome was shown to resemble that of the human proteome in containing many expected nucleolar proteins, ribosomal proteins, and also components of mRNA metabolism, including SR splicing factors. Moreover, an RSZp22-like protein was reported in the nucleolar proteome database (At2g24590; http://germinate.scri.ac.uk/cgi-bin/atnopdb/get-all-data). Furthermore, the authors analyzed the localization of many of these nucleolar proteins identified by proteomic analysis using GFP fusion, 35S promoter, and transient transformation, and 87% of them show different degrees of nucleolar labeling, from weak to strong (Pendle et al., 2005). The authors themselves suggest that the lack of—or weak—nucleolar accumulation of some proteins may be attributable to the protein being either present in low abundance or only transiently associated with the nucleolus at particular cell stages or under certain conditions (Pendle et al., 2005), a situation that could be similar to what we observed for ATP level or kinase activity.

Time-lapse microscopy has revealed that nucleoplasmic proteins can reside transiently within the nucleolus (Sansam et al., 2003). The nucleolar concentration of nucleoplasmic proteins could be a mechanism for sequestering the enzymatic activity from the nucleoplasm (Sansam et al., 2003). More generally, by being the site of transient localization (and/or maturation) of molecules that are involved in nonnucleolar events, the nucleolus might play a role in several cellular processes. On the other hand, RSZp22 may also be involved in several RNA metabolic pathways yet to be defined, occurring in different subnuclear compartments.

Many other splicing molecules have been detected in the nucleolus. The spliceosomal small nuclear RNAs, individually or in the form of the U4/U6.U5 tri-snRNP, are all transiently associated with the nucleolus (Gerbi and Lange, 2002). Recently, it was shown that spliceosomes may preassemble in yeast before binding to pre-mRNA. Furthermore, non-snRNP auxiliary factors have been identified in the sedimentation-based isolated spliceosome particle (Stevens et al., 2002). It has been proposed that the processing/assembly of other RNA–protein edifices, such as the signal recognition particle, occurs within the nucleolus (Politz et al., 2000). It thus remains an open question whether, in higher eukaryotes, the nucleolus is involved in the assembly/maturation of snRNPs involving distinct SR splicing factors. In addition to a

Figure 7. (continued).

Stable transformation of RSp31-GFP in *Arabidopsis* seedlings (**[A]** and **[C]**) and transient RSp31-GFP expression in *Arabidopsis* leaf cells **(B)** are shown.
(A) Low magnification of the primary root expressing RSp31-GFP (left; bars = 200 μm), and high-resolution confocal images of nuclei from trichoblasts of the differentiation zone (bars = 4 μm), atrichoblasts of the elongation zone (bars = 4 μm), and meristematic cells (bars = 2 μm) after α-amanitin, okadaic acid, and staurosporine treatments. Arrowheads show perinucleolar localization of RSp31-GFP.
(B) RSp31-GFP localization in the nucleus of an *Arabidopsis* transiently expressing leaf cell after water treatment as a control and drug treatment: water (far left), α-amanitin (left), okadaic acid (middle), and staurosporine (right).
(C) High-resolution electron microscopic investigation of the nucleus in seedlings treated with water (as a control; top rows) or staurosporine (bottom rows). In nontreated cells, the nucleoli are composed of fibrillar centers (white arrow), dense fibrillar components, and granular components (shown at the periphery of nucleoli by black arrowheads). In treated cells, fibrillar and granular materials (arrows) are visible and are spatially associated with the nucleolus (Nu) in epidermal cells of the root elongation zone (top row) and of the differentiation zone (bottom row). Perinucleolar materials are in direct contact with the nucleolus and can surround electron-dense nucleolus-associated chromatin (right; arrowhead). Serial ultrathin sections (bottom row) demonstrate the spatial importance of the perinucleolar cap-like structure (white arrowheads).

large number of spliceosomal proteins, including SRp20 and RSZp22-related splicing factors (Andersen et al., 2002; Leung et al., 2003; Pendle et al., 2005), human and *Arabidopsis* nucleolar proteomes have revealed components of the exon–exon junction complex involved in mRNA export and nonsense-mediated decay (Pendle et al., 2005). Substantiating this view, *Arabidopsis* ALY proteins that constitute the exon–exon junction complex core have all but one been found localized in the nucleolus (Uhrig et al., 2004). The data presented here noticeably complement the recent proteomic analysis of *Arabidopsis* nucleoli and are indeed consistent with a model in which RSZp22 is dynamically associated with the nucleolus and might also play a role in the mRNA postsplicing metabolic pathway in plants (Pendle et al., 2005).

Our data demonstrate that RSZp22 responds differentially to inhibitor treatments and that its mobility is mainly phosphorylation-dependent. The phosphorylation/dephosphorylation cycle of the RS domain may influence the subnuclear distribution and dynamics of RSZp22, promoting or not the nucleolar localization of the proteins. Intriguingly, we observed similar reorganization and dynamic properties of RSZp22 upon ATP depletion, which might suggest that the absence of RSZp22 mobility upon ATP depletion is linked to its phosphorylation state. ATP depletion could indeed alter many cellular mechanisms, including changes in the phosphorylation levels of proteins and changes in protein interactions (Bhat et al., 1996), which could in turn modulate and modify the dynamic properties of SR proteins.

We were interested in investigating whether another *Arabidopsis* SR protein could associate at least transiently with the nucleolus in a cell type–dependent manner. We took advantage of *Arabidopsis* transgenics expressing RSp31-GFP. We show that, even if phosphorylation inhibition does not promote its nucleolar localization, it induces RSp31 concentration at the nucleolar periphery in cap-like structures, as suggested by electron microscopic analysis. The presence of RSp31 in cap-like structures is a consequence, either directly or indirectly, of the inhibition of kinase activity. Interestingly, such perinucleolar organization of nucleoplasmic RNA binding proteins has been described in animal cells upon transcriptional arrest. In addition, it has been proposed that this is part of a general concerted process of the reorganization of preexisting protein–RNA interactions and newly established interactions (Shav-Tal et al., 2005). It is worth noting that the hypophosphorylated human ASF/SF2 accumulate around the active nucleolar organizing regions at telophase and also at the nucleolar periphery upon transcriptional inhibition (Bubulya et al., 2004). Together, these observations demonstrate striking interrelations between the nucleolar territory, including its periphery, with nucleoplasmic RNA binding proteins and SR splicing factors. The dynamic reorganization of SR splicing factors upon metabolic changes may correspond to complex mechanisms that ensure nuclear functionality.

METHODS

Materials

Arabidopsis thaliana and *Nicotiana tabacum* (cv Petit Havana) seeds were sown on soil in a culture chamber and allowed to germinate and grow under long-day conditions (16-h-light/8-h-dark photoperiod) at ~20°C. *Arabidopsis* plants with well-developed leaf rosettes and 20-cm-high tobacco plants were used for *Agrobacterium tumefaciens*–mediated transient expression as described previously (Tillemans et al., 2005).

Arabidopsis transgenics expressing RSp31 were generated as described previously (Docquier et al., 2004). Transgenic plants (T2 and T3) were selected on plates containing sterile solidified Murashige and Skoog medium supplemented with 3% sucrose and 50 μg/mL glufosinate ammonium (Riedel-de-Haen, Sigma-Aldrich).

Binary Vector Construction and Sequence Analysis

The construction of pBI35S:RSp31-GFP, pBI35S:RSZp22-GFP, and pBI35S:RSZp22ΔRS-GFP has been described in previous reports (Docquier et al., 2004; Tillemans et al., 2005). For the deletion constructs of RSZp22, sequences were amplified directly from pBI35S:RSZp22-GFP by PCR using the proofreading Pfu polymerase (Promega) and specific primers (see Supplemental Table 1 online). The full-length coding regions of GFP-HsfA1, GFP-NLS-CHS-NES_{Rev}, and GFP-NLS-CHS-$NES(-)_{Rev}$ were amplified, respectively, from pRT-GFP-LpHsfA1 (kindly provided by Pascal von Koskull-Döring), pGFP-NLS-CHS-NES, and pGFP-NLS-CHS-NESmut (kindly provided by Thomas Merkle). For all constructs, the fragments were ligated into pBI35S. The resultant plasmids were electroporated into *Agrobacterium* strain GV3101 (pMP90) and were subsequently used for transformations. Independent clones were sequenced to detect any mutation attributable to PCR.

Agrobacterium-Mediated Transformation

Transient transformation was performed essentially as described previously (Tillemans et al., 2005). Briefly, *Agrobacterium* bearing the appropriate binary vector was grown at 28°C overnight in 10 mL of yeast extract broth liquid medium (0.5% sucrose, 0.1% yeast extract, 0.5% bactopeptone, 0.5% Invitrogen beef extract, and 2 mM $MgSO_4$, pH 7.4) supplemented with 25 μg/mL gentamycin, 100 μg/mL rifampicin, and 50 μg/mL kanamycin. After centrifugation, the bacteria were washed with infiltration medium (50 mM MES, 2 mM Na_3PO_4, 0.5% glucose, and 100 μM acetosyringone) and then resuspended in the same medium at the desired final OD_{600}. Leaves were infiltrated using a syringe by applying gentle pressure through the stomata of the abaxial epidermis. The infiltrated areas were cut at different times after inoculation and further processed for imaging or inhibitor treatment. Except for ATP depletion analysis (see below), the study of the localization and dynamics of SR-GFP fusion proteins was kept at <1 h. After this period, a new leaf fragment was cut from the plant and processed for observation.

Confocal Microscopy, Image Analysis, and Photobleaching Experiments

For live cell imaging, a Leica TCS SP2 inverted confocal laser microscope (Leica Microsystems) and a 63× 1.2 numerical aperture Plan-Apo water-immersion objective were used to collect images at 1024 × 1024 pixel resolution. GFP was visualized using the 488-nm line of the argon laser and the RSP500 dichroic mirror. The emission light was dispersed and recorded at 500 to 560 nm. The diameter of the pinhole was set equal to the Airy unit, and we ensured that the maximal fluorescence signal was not saturating the photomultiplier tubes. A series of optical sections were taken to analyze the spatial distribution of fluorescence, and for each nucleus, they were recorded with a Z-step ranging between 0.2 and 0.4 μm. For ribonucleoprotein counterstaining, leaf fragments were incubated for 1 h in 5 μM Syto83 (Molecular Probes). Cells were illuminated with the 488- and 543-nm lines. GFP and Syto83 were detected simultaneously using the 488/543 dichroic mirror, and the Syto83 emission was dispersed and recorded at 550 to 590 nm.

For FRAP experiments, the Leica MicroLab module including Fly-mode was used to analyze very fast kinetics. In this mode, the readout of fluorescence recovery is performed during the x fly-back, providing a time resolution line by line instead of frame by frame between bleach and postbleach images. By analyzing the fluorescence recovery between lines, Fly-mode ensured that the recovery values were as close as possible to the real zero time of the postbleach intensity. For FRAP analysis, the 488-nm laser wavelength was used at 50% laser power and 100% transmission in the photobleaching of the GFP fusion proteins. Nuclei ($n = 5$ to 10 per experiment) were imaged at 256 × 256 pixel medium resolution from at least three independent experiments. Prebleach images (five data points) were acquired by sequentially scanning the same optical section through the nucleus at 3% transmission. Next, a small region of interest was outlined and bleached using the Fly-mode option until the fluorescence was reduced significantly (two to three bleaching iterations). Then, the conditions were set up identically to prebleach settings, and the recovery of fluorescence intensity was monitored every 800 ms by scanning the nucleus until the recovery reached a steady plateau (between 30 and 40 iterations). For quantitative analysis, the postbleach values were normalized to correct for total loss of fluorescence attributable to photobleaching. Relative fluorescence intensity (RFI) was determined as follows: $RFI = (T_0/I_0) \times (I_t/T_t)$, where T_0 is total nuclear intensity before bleaching, T_t is total nuclear intensity at time t, I_0 is average intensity in the region of interest before bleaching, and I_t is average intensity in the region of interest at time t (Phair and Misteli, 2000).

FLIP analyses were performed using the FLIP option within the Leica MicroLab module. For FLIP, a circular region ranging from 1 to 2 μm in either the nucleoplasm or the nucleolus was selected and bleached, and simultaneously, the overall surface of the nucleus (minus the bleached region) was monitored to assess any potential loss of fluorescence from outside the bleached area. Each image collected was of ~1.4 s, and this process was repeated during 100 iterations ($n = 6$). For FLIP shuttling experiments, a large region in the cytoplasm surrounding the nucleus was bleached, as described above, with maximum laser power. The zoom was set to 6 for these FLIP shuttling experiments. We ensured that bleaching did not occur within or too close to the nuclei. Each experiment was repeated at least three times ($n \geq 6$ per experiment).

The values of the bleached (FRAP) and unbleached (FLIP) areas were then normalized and analyzed further using GraphPad Prism 4 and nonlinear regression (GraphPad Software). Captured images were exported as TIFF format files and were further processed using Adobe Photoshop 7.0 for figure mounting and labeling purposes.

Inhibitor Studies and ATP Measurement

Fragments of transiently transformed leaves were used for (de)phosphorylation and transcriptional inhibitor treatments, as described previously (Tillemans et al., 2005). Samples were floated in 10 μM α-amanitin (Sigma-Aldrich), 500 nM okadaic acid (Calbiochem), 50 μM staurosporine (Sigma-Aldrich), or water as a control for various time periods (5 to 15 h). The inhibitor concentrations for *Arabidopsis* transgenic seedlings were 5 μM α-amanitin, 1 μM okadaic acid, and 5 μM staurosporine (Docquier et al., 2004). For LMB treatments, LMB (stock solution at 5 μg/mL in 70% methanol; Sigma-Aldrich) was diluted in water and used at a final concentration of 10 nM. After transformation, leaf cells were treated with LMB (or water as a control) for up to 4 h and were processed for imaging as described below. For ATP depletion, cells were incubated in 3 mM sodium azide (Sigma-Aldrich) and 50 mM 2-deoxyglucose (Sigma-Aldrich) for up to 1 h (the ATP depletion was confirmed using the luciferase assay; see below).

As mentioned in our previous report (Tillemans et al., 2005) and above, an observation period of >2 h leads to an abnormal distribution of SR proteins, possibly because of ATP depletion. To test this hypothesis, leaf fragments were placed in water between slides and cover slips for up to 16 h and then processed for ATP dosage. Leaf fragments ($n = 6$) ground in liquid nitrogen and 5 mL of boiling Tris buffer (50 mM, pH 7.75) were then added. The samples were incubated at 100°C for 10 min. After centrifugation (9500*g* for 4 min at 4°C), ATP level analysis was conducted using the Enliten ATP detection kit according to the manufacturer's protocol (Promega), and luminescence values were measured with the Lumac Biocounter M1500 apparatus.

Electron Microscopy

For electron microscopy, *Arabidopsis* seedlings were fixed in 2% glutaraldehyde (or 2% glutaraldehyde and 2% osmium tetroxide) in phosphate buffer, pH 7.4, and were subsequently processed for Epon embedding. Ultrathin sections were observed with a Zeiss EM900 electron microscope. For the observation of *Arabidopsis* nuclei, serial ultrathin sections were collected on single-slot grids.

Accession Numbers

Data for nucleotide and protein sequences of *Arabidopsis RSZp22* and *RSp31* can be found in the GenBank data library under accession numbers AJ002378 and X99435, respectively.

Supplemental Data

The following materials are available in the online version of this article.

Supplemental Figure 1. Dynamic Distribution of RSZp22-GFP after a Cold Shock and upon ATP Depletion.

Supplemental Figure 2. FLIP-Based Nucleocytoplasmic Shuttling Assay of HsfA1-GFP, GFP-NLS-CHS-NES_{Rev}, and GFP-NLS-CHS-$NES(-)_{Rev}$.

Supplemental Table 1. Primers Used for Vector Constructs (Underlined Letters Show Restriction Enzyme Digestion Sites).

Supplemental Movie 1. Time-Lapse Movie Derived from the FRAP Experiment Shown in Figure 2.

Supplemental Movie 2. Time-Lapse Movie Derived from the FLIP Experiment Shown in Figure 4.

Supplemental Movie 3. Time-Lapse Movie Derived from the FLIP Experiment Shown in Figure 4 upon LMB Treatment.

Supplemental Movie 4. Z-Series Movie Derived from the LMB Treatment Shown in Figure 5.

ACKNOWLEDGMENTS

We thank Pascal von Koskull-Döring (Goethe University) and Thomas Merkle (University of Bielefeld) for kindly providing plasmids. This research was supported by grants from the National Fund for Scientific Research (Grants 2.4520.02, 2.4542.00, 2.4540.06, and 2.4638.05) and from the Fonds Spéciaux du Conseil de la Recherche from the University of Liège. V.T., G.R., and L.D. are doctoral fellows supported by the Fonds de la Recherche pour l'Industrie et l'Agriculture, Belgium.

Received June 2, 2006; revised October 13, 2006; accepted November 1, 2006; published November 17, 2006.

REFERENCES

Ali, G.S., Golovkin, M., and Reddy, A.S. (2003). Nuclear localization and in vivo dynamics of a plant-specific serine/arginine-rich protein. Plant J. **36,** 883–893.

Andersen, J.S., Lyon, C.E., Fox, A.H., Leung, A.K., Lam, Y.W., Steen, H., Mann, M., and Lamond, A.I. (2002). Directed proteomic analysis of the human nucleolus. Curr. Biol. **12,** 1–11.

Angelier, N., Tramier, M., Louvet, E., Coppey-Moisan, M., Savino, T.M., De Mey, J.R., and Hernandez-Verdun, D. (2005). Tracking the interactions of rRNA processing proteins during nucleolar assembly in living cells. Mol. Biol. Cell **16,** 2862–2871.

Azzam, R., Chen, S.L., Shou, W., Mah, A.S., Alexandru, G., Nasmyth, K., Annan, R.S., Carr, S.A., and Deshaies, R.J. (2004). Phosphorylation by cyclin B-Cdk underlies release of mitotic exit activator Cdc14 from the nucleolus. Science **305,** 516–519.

Bernardi, R., Scaglioni, P.P., Bergmann, S., Horn, H.F., Vousden, K.H., and Pandolfi, P.P. (2004). PML regulates p53 stability by sequestering Mdm2 to the nucleolus. Nat. Cell Biol. **6,** 665–672.

Bhat, R., Weaver, J.A., Wagner, C., Bodwell, J.E., and Bresnick, E. (1996). ATP depletion affects the phosphorylation state, ligand binding, and nuclear transport of the 4 S polycyclic aromatic hydrocarbon-binding protein in rat hepatoma cells. J. Biol. Chem. **271,** 32551–32556.

Bourgeois, C.F., Lejeune, F., and Stevenin, J. (2004). Broad specificity of SR (serine/arginine) proteins in the regulation of alternative splicing of pre-messenger RNA. Prog. Nucleic Acid Res. Mol. Biol. **78,** 37–88.

Bouvet, P., Diaz, J.J., Kindbeiter, K., Madjar, J.J., and Amalric, F. (1998). Nucleolin interacts with several ribosomal proteins through its RGG domain. J. Biol. Chem. **273,** 19025–19029.

Bubulya, P.A., Prasanth, K.V., Deerinck, T.J., Gerlich, D., Beaudouin, J., Ellisman, M.H., Ellenberg, J., and Spector, D.L. (2004). Hypophosphorylated SR splicing factors transiently localize around active nucleolar organizing regions in telophase daughter nuclei. J. Cell Biol. **167,** 51–63.

Caceres, J.F., Misteli, T., Screaton, G.R., Spector, D.L., and Krainer, A.R. (1997). Role of the modular domains of SR proteins in subnuclear localization and alternative splicing specificity. J. Cell Biol. **138,** 225–238.

Caceres, J.F., Screaton, G.R., and Krainer, A.R. (1998). A specific subset of SR proteins shuttles continuously between the nucleus and the cytoplasm. Genes Dev. **12,** 55–66.

Catez, F., Erard, M., Schaerer-Uthurralt, N., Kindbeiter, K., Madjar, J.J., and Diaz, J.J. (2002). Unique motif for nucleolar retention and nuclear export regulated by phosphorylation. Mol. Cell. Biol. **22,** 1126–1139.

Cazalla, D., Newton, K., and Caceres, J.F. (2005). A novel SR-related protein is required for the second step of pre-mRNA splicing. Mol. Cell. Biol. **25,** 2969–2980.

Chen, D., and Huang, S. (2001). Nucleolar components involved in ribosome biogenesis cycle between the nucleolus and nucleoplasm in interphase cells. J. Cell Biol. **153,** 169–176.

Creancier, L., Prats, H., Zanibellato, C., Amalric, F., and Bugler, B. (1993). Determination of the functional domains involved in nucleolar targeting of nucleolin. Mol. Biol. Cell **4,** 1239–1250.

Docquier, S., Tillemans, V., Deltour, R., and Motte, P. (2004). Nuclear bodies and compartmentalization of pre-mRNA splicing factors in higher plants. Chromosoma **112,** 255–266.

Dundr, M., and Misteli, T. (2001). Functional architecture in the cell nucleus. Biochem. J. **356,** 297–310.

Fang, Y., Hearn, S., and Spector, D.L. (2004). Tissue-specific expression and dynamic organization of SR splicing factors in Arabidopsis. Mol. Biol. Cell **15,** 2664–2673.

Gao, H., Gordon-Kamm, W.J., and Lyznik, L.A. (2004). ASF/SF2-like maize pre-mRNA splicing factors affect splice site utilization and their transcripts are alternatively spliced. Gene **339,** 25–37.

Gendra, E., Moreno, A., Alba, M.M., and Pages, M. (2004). Interaction of the plant glycine-rich RNA-binding protein MA16 with a novel nucleolar DEAD box RNA helicase protein from *Zea mays.* Plant J. **38,** 875–886.

Gerbi, S.A., and Lange, T.S. (2002). All small nuclear RNAs (snRNAs) of the [U4/U6.U5] tri-snRNP localize to nucleoli: Identification of the nucleolar localization element of U6 snRNA. Mol. Biol. Cell **13,** 3123–3137.

Graveley, B.R. (2000). Sorting out the complexity of SR protein functions. RNA **6,** 1197–1211.

Haasen, D., Kohler, C., Neuhaus, G., and Merkle, T. (1999). Nuclear export of proteins in plants: AtXPO1 is the export receptor for leucine-rich nuclear export signals in *Arabidopsis thaliana.* Plant J. **20,** 695–705.

Heerklotz, D., Doring, P., Bonzelius, F., Winkelhaus, S., and Nover, L. (2001). The balance of nuclear import and export determines the intracellular distribution and function of tomato heat stress transcription factor HsfA2. Mol. Cell. Biol. **21,** 1759–1768.

Huang, Y., Gattoni, R., Stevenin, J., and Steitz, J.A. (2003). SR splicing factors serve as adapter proteins for TAP-dependent mRNA export. Mol. Cell **11,** 837–843.

Huang, Y., and Steitz, J.A. (2001). Splicing factors SRp20 and 9G8 promote the nucleocytoplasmic export of mRNA. Mol. Cell **7,** 899–905.

Huang, Y., and Steitz, J.A. (2005). SRprises along a messenger's journey. Mol. Cell **17,** 613–615.

Huang, Y., Yario, T.A., and Steitz, J.A. (2004). A molecular link between SR protein dephosphorylation and mRNA export. Proc. Natl. Acad. Sci. USA **101,** 9666–9670.

Igarashi, D., Ishida, S., Fukazawa, J., and Takahashi, Y. (2001). 14-3-3 proteins regulate intracellular localization of the bZIP transcriptional activator RSG. Plant Cell **13,** 2483–2497.

Isshiki, M., Tsumoto, A., and Shimamoto, K. (2006). The serine/arginine-rich protein family in rice plays important roles in constitutive and alternative splicing of pre-mRNA. Plant Cell **18,** 146–158.

Jurica, M.S., and Moore, M.J. (2003). Pre-mRNA splicing: Awash in a sea of proteins. Mol. Cell **12,** 5–14.

Kalyna, M., and Barta, A. (2004). A plethora of plant serine/arginine-rich proteins: Redundancy or evolution of novel gene functions? Biochem. Soc. Trans. **32,** 561–564.

Kruhlak, M.J., Lever, M.A., Fischle, W., Verdin, E., Bazett-Jones, D.P., and Hendzel, M.J. (2000). Reduced mobility of the alternate splicing factor (ASF) through the nucleoplasm and steady state speckle compartments. J. Cell Biol. **150,** 41–51.

Lai, M.C., and Tarn, W.Y. (2004). Hypophosphorylated ASF/SF2 binds TAP and is present in messenger ribonucleoproteins. J. Biol. Chem. **279,** 31745–31749.

Lamond, A.I., and Spector, D.L. (2003). Nuclear speckles: A model for nuclear organelles. Nat. Rev. Mol. Cell Biol. **4,** 605–612.

Lazar, G., and Goodman, H.M. (2000). The Arabidopsis splicing factor SR1 is regulated by alternative splicing. Plant Mol. Biol. **42,** 571–581.

Lemaire, R., Prasad, J., Kashima, T., Gustafson, J., Manley, J.L., and Lafyatis, R. (2002). Stability of a PKCI-1-related mRNA is controlled by the splicing factor ASF/SF2: A novel function for SR proteins. Genes Dev. **16,** 594–607.

Leung, A.K., Andersen, J.S., Mann, M., and Lamond, A.I. (2003). Bioinformatic analysis of the nucleolus. Biochem. J. **376,** 553–569.

Lippincott-Schwartz, J., Snapp, E., and Kenworthy, A. (2001). Studying protein dynamics in living cells. Nat. Rev. Mol. Cell Biol. **2,** 444–456.

Liu, K., Li, L., and Luan, S. (2005a). An essential function of phosphatidylinositol phosphates in activation of plant shaker-type K^+ channels. Plant J. **42,** 433–443.

Liu, Y., Randall, W.R., and Schneider, M.F. (2005b). Activity-dependent and -independent nuclear fluxes of HDAC4 mediated by different kinases in adult skeletal muscle. J. Cell Biol. **168,** 887–897.

Lopato, S., Forstner, C., Kalyna, M., Hilscher, J., Langhammer, U., Indrapichate, K., Lorkovic, Z.J., and Barta, A. (2002). Network of interactions of a novel plant-specific Arg/Ser-rich protein, atRSZ33, with atSC35-like splicing factors. J. Biol. Chem. **277,** 39989–39998.

Lopato, S., Gattoni, R., Fabini, G., Stevenin, J., and Barta, A. (1999a). A novel family of plant splicing factors with a Zn knuckle motif: Examination of RNA binding and splicing activities. Plant Mol. Biol. **39,** 761–773.

Lopato, S., Kalyna, M., Dorner, S., Kobayashi, R., Krainer, A.R., and Barta, A. (1999b). atSRp30, one of two SF2/ASF-like proteins from *Arabidopsis thaliana*, regulates splicing of specific plant genes. Genes Dev. **13,** 987–1001.

Lopato, S., Waigmann, E., and Barta, A. (1996). Characterization of a novel arginine/serine-rich splicing factor in Arabidopsis. Plant Cell **8,** 2255–2264.

Lorkovic, Z.J., Hilscher, J., and Barta, A. (2004). Use of fluorescent protein tags to study nuclear organization of the spliceosomal machinery in transiently transformed living plant cells. Mol. Biol. Cell **15,** 3233–3243.

Matlin, A.J., Clark, F., and Smith, C.W. (2005). Understanding alternative splicing: Towards a cellular code. Nat. Rev. Mol. Cell Biol. **6,** 386–398.

Mekhail, K., Khacho, M., Carrigan, A., Hache, R.R., Gunaratnam, L., and Lee, S. (2005). Regulation of ubiquitin ligase dynamics by the nucleolus. J. Cell Biol. **170,** 733–744.

Melcak, I., Cermanova, S., Jirsova, K., Koberna, K., Malinsky, J., and Raska, I. (2000). Nuclear pre-mRNA compartmentalization: Trafficking of released transcripts to splicing factor reservoirs. Mol. Biol. Cell **11,** 497–510.

Misteli, T. (2000). Cell biology of transcription and pre-mRNA splicing: Nuclear architecture meets nuclear function. J. Cell Sci. **113,** 1841–1849.

Misteli, T., Caceres, J.F., Clement, J.Q., Krainer, A.R., Wilkinson, M.F., and Spector, D.L. (1998). Serine phosphorylation of SR proteins is required for their recruitment to sites of transcription in vivo. J. Cell Biol. **143,** 297–307.

Misteli, T., Caceres, J.F., and Spector, D.L. (1997). The dynamics of a pre-mRNA splicing factor in living cells. Nature **387,** 523–527.

Moriguchi, K., Suzuki, T., Ito, Y., Yamazaki, Y., Niwa, Y., and Kurata, N. (2005). Functional isolation of novel nuclear proteins showing a variety of subnuclear localizations. Plant Cell **17,** 389–403.

Patel, A.A., and Steitz, J.A. (2003). Splicing double: Insights from the second spliceosome. Nat. Rev. Mol. Cell Biol. **4,** 960–970.

Pederson, T. (1998). The plurifunctional nucleolus. Nucleic Acids Res. **26,** 3871–3876.

Pendle, A.F., Clark, G.P., Boon, R., Lewandowska, D., Lam, Y.W., Andersen, J., Mann, M., Lamond, A.I., Brown, J.W., and Shaw, P.J. (2005). Proteomic analysis of the Arabidopsis nucleolus suggests novel nucleolar functions. Mol. Biol. Cell **16,** 260–269.

Phair, R.D., and Misteli, T. (2000). High mobility of proteins in the mammalian cell nucleus. Nature **404,** 604–609.

Pih, K.T., Yi, M.J., Liang, Y.S., Shin, B.J., Cho, M.J., Hwang, I., and Son, D. (2000). Molecular cloning and targeting of a fibrillarin homolog from Arabidopsis. Plant Physiol. **123,** 51–58.

Politz, J.C., Yarovoi, S., Kilroy, S.M., Gowda, K., Zwieb, C., and Pederson, T. (2000). Signal recognition particle components in the nucleolus. Proc. Natl. Acad. Sci. USA **97,** 55–60.

Sacco-Bubulya, P., and Spector, D.L. (2002). Disassembly of interchromatin granule clusters alters the coordination of transcription and pre-mRNA splicing. J. Cell Biol. **156,** 425–436.

Sanford, J.R., Ellis, J.D., Cazalla, D., and Caceres, J.F. (2005). Reversible phosphorylation differentially affects nuclear and cytoplasmic functions of splicing factor 2/alternative splicing factor. Proc. Natl. Acad. Sci. USA **102,** 15042–15047.

Sanford, J.R., Gray, N.K., Beckmann, K., and Caceres, J.F. (2004). A novel role for shuttling SR proteins in mRNA translation. Genes Dev. **18,** 755–768.

Sansam, C.L., Wells, K.S., and Emeson, R.B. (2003). Modulation of RNA editing by functional nucleolar sequestration of ADAR2. Proc. Natl. Acad. Sci. USA **100,** 14018–14023.

Scherl, A., Coute, Y., Deon, C., Calle, A., Kindbeiter, K., Sanchez, J.C., Greco, A., Hochstrasser, D., and Diaz, J.J. (2002). Functional proteomic analysis of human nucleolus. Mol. Biol. Cell **13,** 4100–4109.

Shav-Tal, Y., Blechman, J., Darzacq, X., Montagna, C., Dye, B.T., Patton, J.G., Singer, R.H., and Zipori, D. (2005). Dynamic sorting of nuclear components into distinct nucleolar caps during transcriptional inhibition. Mol. Biol. Cell **16,** 2395–2413.

Stevens, S.W., Ryan, D.E., Ge, H.Y., Moore, R.E., Young, M.K., Lee, T.D., and Abelson, J. (2002). Composition and functional characterization of the yeast spliceosomal penta-snRNP. Mol. Cell **9,** 31–44.

Thiry, M., and Lafontaine, D.L. (2005). Birth of a nucleolus: The evolution of nucleolar compartments. Trends Cell Biol. **15,** 194–199.

Tillemans, V., Dispa, L., Remacle, C., Collinge, M., and Motte, P. (2005). Functional distribution and dynamics of Arabidopsis SR splicing factors in living plant cells. Plant J. **41,** 567–582.

Tsai, R.Y., and McKay, R.D. (2005). A multistep, GTP-driven mechanism controlling the dynamic cycling of nucleostemin. J. Cell Biol. **168,** 179–184.

Uhrig, J.F., Canto, T., Marshall, D., and MacFarlane, S.A. (2004). Relocalization of nuclear ALY proteins to the cytoplasm by the tomato bushy stunt virus P19 pathogenicity protein. Plant Physiol. **135,** 2411–2423.

van den Boom, V., Citterio, E., Hoogstraten, D., Zotter, A., Egly, J.M., van Cappellen, W.A., Hoeijmakers, J.H., Houtsmuller, A.B., and Vermeulen, W. (2004). DNA damage stabilizes interaction of CSB with the transcription elongation machinery. J. Cell Biol. **166,** 27–36.

van Der Houven Van Oordt, W., Newton, K., Screaton, G.R., and Caceres, J.F. (2000). Role of SR protein modular domains in alternative splicing specificity in vivo. Nucleic Acids Res. **28,** 4822–4831.

Ward, B.M., and Lazarowitz, S.G. (1999). Nuclear export in plants. Use of geminivirus movement proteins for a cell-based export assay. Plant Cell **11,** 1267–1276.

Weingartner, M., Binarova, P., Drykova, D., Schweighofer, A., David, J.P., Heberle-Bors, E., Doonan, J., and Bogre, L. (2001). Dynamic recruitment of Cdc2 to specific microtubule structures during mitosis. Plant Cell **13,** 1929–1943.

Yanovsky, M.J., Luppi, J.P., Kirchbauer, D., Ogorodnikova, O.B., Sineshchekov, V.A., Adam, E., Kircher, S., Staneloni, R.J., Schafer, E., Nagy, F., and Casal, J.J. (2002). Missense mutation in the PAS2 domain of phytochrome A impairs subnuclear localization and a subset of responses. Plant Cell **14,** 1591–1603.

Zemach, A., Li, Y., Ben-Meir, H., Oliva, M., Mosquna, A., Kiss, V., Avivi, Y., Ohad, N., and Grafi, G. (2006). Different domains control the localization and mobility of LIKE HETEROCHROMATIN PROTEIN1 in *Arabidopsis* nuclei. Plant Cell **18,** 133–145.

Zhang, Z., and Krainer, A.R. (2004). Involvement of SR proteins in mRNA surveillance. Mol. Cell **16,** 597–607.

Zirwes, R.F., Kouzmenko, A.P., Peters, J.M., Franke, W.W., and Schmidt-Zachmann, M.S. (1997). Topogenesis of a nucleolar protein: Determination of molecular segments directing nucleolar association. Mol. Biol. Cell **8,** 231–248.